Saudi Journal of Biological Sciences 27 (2020) 3113–3124

Contents lists available at ScienceDirect

Saudi Journal of Biological Sciences

journal homepage: www.sciencedirect.com

Original article

Verbesina crocata: A pharmacognostic study for the treatment of wound healing

Ana María García-Bores [a,*], Nallely Álvarez-Santos [a,e], Ma. Edith López-Villafranco [b], María Patricia Jácquez-Ríos [b], Silvia Aguilar-Rodríguez [c], Dalia Grego-Valencia [c], Adriana Montserrat Espinosa-González [a], Edgar Antonio Estrella-Parra [a], Claudia Tzasná Hernández-Delgado [a], Rocío Serrano-Parrales [a], María del Rosario González-Valle [d], José del Carmen Benítez-Flores [d]

[a] *Laboratorio de Fitoquímica, UBIPRO, Facultad de Estudios Superiores-Iztacala, Universidad Nacional Autónoma de México, Av. De los Barrios No. 1, Los Reyes Iztacala, Tlalnepantla 54090, Estado de Mexico, Mexico*
[b] *Herbario IZTA, Facultad de Estudios Superiores Iztacala, Universidad Nacional Autónoma de México, Av. De los Barrios No. 1, Los Reyes Iztacala, Tlalnepantla 54090, Estado de Mexico, Mexico*
[c] *Laboratorio de Botánica, UMF, Facultad de Estudios Superiores Iztacala, Universidad Nacional Autónoma de México, Av. De los Barrios No. 1, Los Reyes Iztacala, Tlalnepantla 54090, Estado de Mexico, Mexico*
[d] *Laboratorio 1 de Histología, UMF, Facultad de Estudios Superiores-Iztacala, Universidad Nacional Autónoma de México, Av. De los Barrios No. 1, Los Reyes Iztacala, Tlalnepantla 54090, Estado de Mexico, Mexico*
[e] *Posgrado en Ciencias Biológicas, Unidad de Posgrado, Edificio D, Primer Piso, Oficina D-101, Ciudad Universitaria, Universidad Nacional Autónoma de México, Circuito de Posgrados s/n, Alcaldía Coyoacán 04510, CDMX, Mexico*

ARTICLE INFO

Article history:
Received 22 April 2020
Revised 23 August 2020
Accepted 26 August 2020
Available online 2 September 2020

Keywords:
Verbesina crocata
Plant anatomy
Antioxidant properties
Catechin derivates
Wound healing

ABSTRACT

Ethnopharmacological relevance: *Verbesina crocata* (Cav.) Less. (Arnica or Capitaneja) is an endemic plant from Mexico restricted to the western part of the country. The aerial parts are used in traditional medicine for the treatment of wounds and burns. The objective of this investigation was to carry out a pharmacognostic study of *V. crocata* and establish markers that allow for the recognition of the characteristics of the plant and validate its traditional use. The study includes anatomical and chemical characteristics of the plant as well as evaluations of its antioxidant capacity and wound healing ability in a murine model.
Materials and methods: An anatomical study of *V. crocata* was performed on the middle part of the leaf and stem. A methanolic extract of this species (VcME) was obtained by methanolic maceration of the aerial parts. Subsequently, a partition of the VcME was made to obtain a hexanic fraction (VcH). The phytochemical preliminary screening and characterization by high-performance liquid chromatography/mass spectrometry (HPLC-ESI/MS) of the VcME and VcH were performed. The antioxidant activity and total phenolic content were quantified. The wound healing capacity of the methanolic extract was determined in CD-1 mice by the healing rate, the tensiometric method, and histological analysis.
Results: The anatomical study of *V. crocata* showed the presence of two types of secretory structures and their position on the leaves. In addition, the characteristics of the middle vein and trichomes are potentially useful for recognition of the species. Chemical compounds detected by HPLC-ESI/MS reveal the presence of sitosterol glycoside and catechin derivatives as principal constituents of *V. crocata*. The VcME showed low antioxidant capacity and total phenolic. *V. crocata* had a similar healing effect to Recoveron® in the tensiometric method, but the rate of healing was higher. According to the histological

* Corresponding author.
E-mail addresses: boresana@iztacala.unam.mx (A.M. García-Bores), edithlov@iztacala.unam.mx (M.E. López-Villafranco), siagro@unam.mx (S. Aguilar-Rodríguez), tzasna@unam.mx (C.T. Hernández-Delgado).

Peer review under responsibility of King Saud University.

Production and hosting by Elsevier

https://doi.org/10.1016/j.sjbs.2020.08.038

analysis, the treatment of *V. crocata* promoted the remodelling phase 15 days after the incisional wound. *Conclusion:* This is the first pharmacognostic study of this species that covers the plant anatomy, chemical content and biological properties related to its traditional use. *V. crocata* favours wound healing according to physical and histological evaluations. In addition, the characteristics of the middle vein, trichomes and catechin glycosides are potentially useful for the recognition of this species.

1. Introduction

Wound healing is a complex and dynamic process that re-establishes the integrity of damaged tissue. Normal wound healing involves four successive and overlapping phases (Wang et al., 2018). After a wound: (a) begins the phase of haemostasis, where the exposed sub-endothelium secretes factors that induce clot formation; (b) in the inflammatory phase, the wound is debrided for leukocytes; (c) the proliferative phase is characterized by the presence of tissue of granulation formed by extracellular matrix (ECM) to replace the originally formed clot. Subsequently, contraction of the wound area and epithelialization occurs; (d) finally, in the remodelling phase connective tissue is formed with the gradual degradation of the ECM, and immature collagen type III is replaced with the mature type I collagen fibres, which increases the tensile strength and establishment of the newly formed epithelium (Ali et al., 2019). Deregulation of any of these phases results in impaired healing, e.g., chronic ulcers or excessive scarring (Landén et al., 2016).

Plants positively affect wound healing (Biswas et al., 2017; Sathyanarayanan et al., 2017; Song et al., 2017). Medicinal plants are beneficial for wound treatment, promoting the rate of scarring and reducing scar formation in patients (Kumar et al., 2007; Chitra et al., 2009).

Verbesina crocata (Cav.) Less. (Asteraceae) is known as ‘‘arnica” or ‘‘capitaneja”. The aerial part is prepared in the form of tea or an infusion for the treatment of wounds and burns by the inhabitants of San Rafael Coxcatlán in the Tehuacán-Cuicatlán Valley, Puebla State, Mexico (Canales et al., 2005). The inhabitants usually have the plant in their home gardens for the treatment of wounds, burns and other sufferings. In the states of Nayarit to Veracruz, Morelos, State of Mexico, Guerrero, Oaxaca, this plant is use as antidiabetic, diuretic, diaphoretic, anti-pyretic, astringent, aphrodisiac and for illnesses of eyes. The part of the plant used are flowers and leaves (Pérez et al., 1984). Also, Alonso-Castro et al. (2011) reported that *V. crocata* is used for dermatological conditions.

V. crocata is an endemic plant in Mexico that is restricted to the western part of the country (Olsen, 1988). Taxonomically, this species is as follows: shrub; stems with wings from 1 to 5 mm wide, hispidulous; leaves asperous, opposite, 10 to 16 cm long by 5 to 8 cm wide, deltoid, entire or lobate, the margins dentate, apex acuminate, base decurrent; inflorescence paniculate, discoid heads 1–5, peduncle up to 20 cm long, involucre with lanceolate bracts, external ones shorter than internal ones; flowers orange, 7 mm long; achene winged, obovate, 5.5 to 8 mm long by 3.5 to 4.5 mm wide (Vibrans, 2011). However, the anatomical characteristics of the leaves and stems have not been established for this species.

There are few reports on the biological properties of *V. crocata*. These are related to the hypoglycaemic (Marles and Farnsworth, 1995; Andrade-Cetto and Heinrich, 2005), diuretic effect (Salazar-Gómez et al., 2018) and anti-inflammatory activity (Rodríguez, 2014) of the plant in animal models. However, there are no studies on the effect of *V. crocata* on wound healing.

The aim of this research was to conduct a pharmacognostic study of *V. crocata* that includes the vegetative anatomy (leaf and stem), the chemical characterization, the evaluation of its antioxidant and the wound healing capacity in a murine model related to its traditional use.

2. Methods and materials

2.1. Plant material and extraction

The aerial parts (stems and leaves) of *V. crocata* (Cav.) Less. (Asteraceae) were collected in July 2016 in San José Tilapa, Coxcatlán (Puebla, Mexico), in the Tehuacán-Cuicatlán Valley, at 18°09′40.4″ north latitude, 97°06′11.9″ west longitude and 917 m.a.s.l. The plant was deposited at the Izta Herbarium of Universidad Nacional Autónoma de México, where a voucher specimen was registered with No. 2528 IZTA (Fig. 1A). The plant name has been checked with ‘‘The Plant List 2013” (http://www.theplantlist.org/tpl1.1/search?q=Verbesina+crocata).

Three individuals of *V. crocata* were used for the anatomical study from the same set of plants employed for phytochemical analysis.

The aerial parts of *V. crocata* were ground to a powder (425 g). The powder was extracted by maceration with methanol (VcME) for one week, three consecutive times. The extract was filtered and concentrated under reduced pressure. The yield of VcME was calculated by the ratio of the solids obtained and the mass of plant material used for the extraction (% w/w). Then, one part of the VcME was partitioned with hexane to obtain the hexanic fraction (VcH).

2.2. Anatomical study of V. crocata

The anatomical study was performed on the middle part of the stem and leaf (blade and petiole). The anatomical characteristics of the leaf and stem of *V. crocata* were compared with the reports of other species of the genus to determine the differences between the species and to propose useful taxonomic attributes in the characterization of the plant.

A free-hand sectioning method was carried out, some tissues were cleared with sodium hydroxide and sodium hypochlorite; stained and mounted in glycerine jelly with safranin (Aguilar-Rodríguez, 1998). To detect the presence of lipids, some tissues were stained with Sudan IV. Other samples were processed by the paraffin inclusion method (Ruzin, 1999); subsequently, cross-sections of 15 μm thickness were obtained using a rotary microtome (Leica SM2010R). Tissue staining was performed with safranin-fast green (Johansen, 1940). Finally, the sections were mounted in synthetic resin. Images and measurements were obtained with the NIS-Elements BR software (version 3.2) provide by Nikon Instruments. Anatomical descriptions were made according to Metcalfe and Chalk (1950, 1979) and Fahn (1985).

2.3. Phytochemical composition of V. crocata

2.3.1. Phytochemical screening

Preliminary phytochemical screening was performed. The VcME and VcH were analysed for different phytoconstituents, including steroids and terpenoids (Lieberman-Burchard test), sesquiterpene lactones (Baljet test), alkaloids (Dragendorff and Mayer tests), phe-

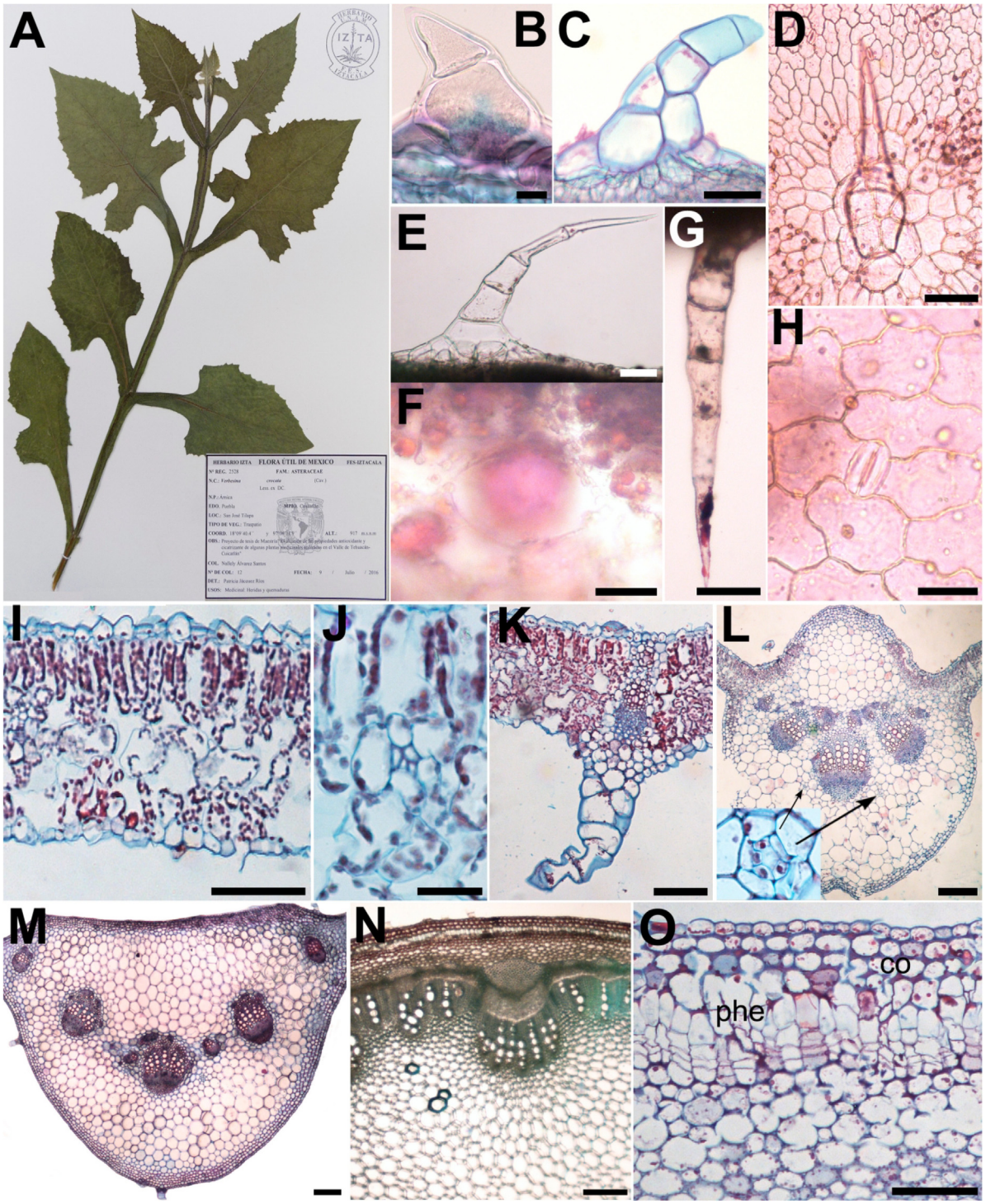

Fig. 1. *V. crocata* anatomy. A. Morphology, herbarium voucher; B-M. Leaf characters. B. short cylindrical shape trichome; C–E and G. Uniseriate trichomes with 2–5 cells; F. Oil-secretory cavity; H. Anomocytic stomata; I. Leaf cross section; J. Oil-secretory ducts; K. Collateral vascular bundles; L. Biconvex middle vein, Oil-secretory ducts close-up; M. Petiole cross section; N-O. Stem characters. N. General cross view; and O. Periderm and collenchyma in detail. co: collenchyma; phe: phellema.

nols (ferric chloride test), glycosides (Molisch test) by the usually prescribed chromogenic reactions and saponins (foam test) (Gautam et al., 2010).

2.3.2. High-performance liquid chromatography-diode array detector-electrospray ionization/mass spectrometry (HPLC-DAD-ESI/MS)

The chemical analysis of the VcME and VcH was performed by HPLC-DAD-ESI/MS. The HPLC apparatus (Thermo Dionex Ultimate 3000) consisted of a diode array with UV-ESI/MS detection. Chromeleon Software was used. The system consisted of a PDA detector (at 254–350 nm). The column was a Nucleodex β-OH (Macherey Nagel 720124, 200 mm × 4 mm, 5 μm). The samples were analysed using a gradient of 0.1% formic acid in water (v/v) (A), 0.1% formic acid in acetonitrile (v/v) (B) and 0.1% acid formic in methanol (v/v) (C): starting with 95% A, 10% B and 10% C and ending after 30 min with 43% B and 57% C. 40 μL of each sample (1 mg/mL) was

injected. The flow rate was 0.6 mL/min, and a quaternary 600 pump connected to an autosampler was cooled to 20 °C.

An Orbitrap Fusion Tri-hybrid system was used with an ESI source controlled by Xcalibur Software (Thermo Scientific Xcalibur V. 4.1.5.0). The operating parameters were as follows: ion transfer tube temp 260 °C; vaporizer temp 350 °C; detector type: ion trap; use quadrupole isolation: true; scan range 50–1000 (*m*/*z*); polarity: positive; intensity threshold: 5.0e4; mass range 50–1000 (*m*/*z*); isolation mode: quadrupole; HCD collision energy 35%; first mass 50 (*m*/*z*); AGC target: 5.0e4. Nitrogen and helium of ultra-high purity were used as nebulizing gases. The experimental conditions for the analysis $ddMS^2$ and $ddMS^3$ are in the supplementary material.

The following compounds were used as standard to compare their fragmentation patterns with the experimental ones: catechin (C1251), quercetin (Q0125), gallic acid (G7384) and shikimic acid (S5375). All standard compounds were purchased from Sigma-Aldrich.

Also, the experimental spectral were compared with the Spectral Database for Organic Compounds (SDBS) and the National Institute of standards and technology (NIST, 2017).

2.4. DPPH and ABTS radicals-scavenging capacity and total phenol content of VcME

The scavenging of 1,1-diphenyl-2-picrylhydrazyl free radicals (DPPH) was measured using modification of the method of López-Alarcón and Denicola, 2013. Quercetin and catechin were used as positive controls. Quercetin and catechin (1–10 μg/mL), DPPH (250 mM) and VcME (10–500 μg/mL) were dissolved in MeOH. At least six different dilutions of the extract were tested and allowed to incubate for 30 min in the dark before the absorbance was measured at 515 nm in an ELISA spectrophotometer (Multiskan FC, Thermo Scientific). The experiment was conducted in triplicate. The scavenging activity of each concentration was calculated as a percent of the reduction of the DPPH concentration as follows:

$$\%\ \text{Reduction} = [(\text{Abs DPPH} - \text{Abs Sample})/\text{Abs DPPH}] \times 100$$

where Abs DPPH is the absorbance of DPPH in MeOH and Abs Sample represents the absorbance of each sample in the presence of each concentration of VcME, catechin or quercetin.

The antioxidant activity was expressed as an IC_{50} value (μg/mL), the inhibitory concentration of the sample or positive control necessary to reduce the absorbance of DPPH by 50% compared to the negative control. A lower IC_{50} value represents a higher antioxidant activity.

ABTS radical-scavenging capacity. The 2,2′-azino-bis-(3-ethyl benzothiazoline-6-sulphonic acid) radical cation (ABTS) scavenging activity of VcME was examined according to the method proposed by Re et al. (1999). Calibration curves were prepared using different volumes of a standard quercetin and catechin solution (1.5–15 μg/mL) as positive controls and VcME (100–1000 μg/mL) as the test. The antioxidant capacity was expressed as an IC_{50} value (μg/mL). Each test was run at least in triplicate.

The total polyphenol content of VcME was determined using Folin–Ciocalteu's phenol reagent according to a method described previously (Mandalari et al., 2010). The total polyphenols were expressed as mg of gallic acid equivalents per gram of extract (mg GAE/g extract). A standard curve was constructed with different concentrations of gallic acid (2–10 μg/mL). The solutions of gallic acid and VcME (500 μg/mL) were prepared in MeOH-water.

2.5. Wound healing activity

The parameters used to evaluate the wound healing activity of VcME were: (a) the wound closing speed (WCS, mm/day), (b) the final closing time (FCT, day) (c) the resistance of the skin to the tensile force necessary to open the wound expressed in grams (Rozaini et al., 2004); this last parameter is an important measure since it reflects the subdermal organization of the newly synthesized collagen fibres in the healing process; and (d) Histological analysis was also carried out to determine which phase of skin healing the samples were in as well as the organization of the collagen, the size of the healed wound (SHW) and the quantification of fibroblasts in the SHW.

2.5.1. Experimental animals and the protocol of wound healing activity

Male CD-1 mice (*Mus musculus*) 6–8 weeks of age from FES-Iztacala Bioterium, UNAM, were employed and maintained in a climate-controlled environment with a 12 h light/dark cycle. Five mice were housed per cage and acclimatized for two weeks before starting the experiment. Throughout the experimental period, mice had free access to food and water that were provided through the food chamber on top of the cages. The Bioethical Committee/FES Iztacala, UNAM approved all animal protocols according to NOM-062-ZOO-1999.

Wound healing activity was performed using the tensiometric method based on measuring wound resistance to tension (Rozaini et al., 2004). The experimental groups were as follows: 1) C- negative control: Vaseline® as a vehicle (Unilever, Trumbull CT 06611, EUA); 2) C+ positive control: Recoveron® (sodium acexamate in ointment; Armstrong, Mexico); 3) VcME (5% w/w in Vaseline®). The VcME was incorporated into Vaseline® according to the method proposed previously by Block (2013). The petroleum jelly was melted to facilitate the handling and dispersion of VcME. The formulation is cooled slowly, using continuous stirring to maintain dispersion.

The back of the mice was depilated (Nair® sensitive skin). 24 h later, the mice were anaesthetized (99.9% isoflurane 100 μL/-mouse). An incisional wound 1.5 cm in length was made. The wound remained without any kind of cover. Subsequently, the different treatments were applied every 24 h for 14 consecutive days (Rozaini et al., 2004). The dorsal areas of the mice were monitored daily to see if there were any signs of any signs of irritation like or inflammation or skin alteration like erythema, oedema, ulcers, etc (Chew and Maibach, 2006).

The length of the wound was measured during the 14 days of treatment and including the day of sacrifice (digital Vernier Surtek®) (Gupta and Jain, 2011). With these data, the rate of healing was determined by calculating the WCS of each treatment (mm/day). The time in days when the wound macroscopically closed was also recorded (FCT).

After completing 14 days of treatment, the animals were sacrificed by asphyxiation in a CO_2 chamber. Then, the tension force (g) necessary to open the wounds was measured. For this, calibrated dynamometers of 500 and 1000 g were used (Ohaus 01710 and 01740, respectively). The results were reported as the tensile strength represented as grams.

2.5.2. Histological analysis

For this study, the histological evolution of the healing process was performed in parallel to that of the tensiometer with the same characteristics: groups/treatments, wound size, measures of the length of the wound and sacrifice with CO_2. After the mice were sacrificed, skin samples for histological analysis were taken from the area of the wound (1 cm^2) and adjacent-normal skin approximately 2 cm to the periphery of the wound.

The dorsal skin samples were fixed in 2% (w/v) paraformaldehyde PBS buffer solution (pH 7.2) for 24 h, dehydrated with a sequence of ethanol solutions (70, 80, 95 96 and 100% v/v), cleared with two changes of xylol and finally included in paraffin. The skin samples were cut in half to obtain the distal and the middle parts of the wound for inclusion. Then, the samples were sectioned at 3 μm and stained with haematoxylin and eosin (H&E); and Masson's trichrome staining (MT).

Histological changes in each section were observed using multiple microscopic fields and photographed with a photomicroscope (Leica DM 5000). Normal skin in each group received topical application of the treatments. The histological appearance of these samples was normal in all mice. Therefore, none of the treatments showed evidence of skin irritation.

Histological diagnosis was performed by comparing the normal skin with the distal and middle samples from the wound of the C-, C+ and VcME groups. The area of the wound was classified as small (0.21–0.60 μm), medium (0.61–1.20 μm), or large (1.21–2.00 μm) considering the size of the healed wound (SWH) or regeneration. For the quantification of fibroblasts in SHW, histological observations were made in seven-images view 1000X objective magnification. The results are presented as the average fibroblasts per mouse in each treatment (Dwita et al., 2019). Additionally, the neoformation of epidermal granulation tissue, neoformation and congestion of vessels, and collagen fibres (thickness, disposition, mature and immature collagen) were considered to determine the effect of each treatment in the phases of the healing process: haemostasis/inflammatory, proliferative and remodelling (Gantwerker and Hom, 2012).

2.6. Statistical analysis

Shapiro-Wilk's test was performed to verify the normality of the data on the antioxidant and wound healing activity (tensiometric method) and quantification of fibroblasts. Experiments to determine the DPPH and ABTS radicals scavenging capacity and total phenol content were performed in triplicate. The IC_{50} values were calculated by a linear model. The wound healing activity was considered as n = 5. The results were analysed with a one-way analysis of variance (ANOVA). For the closure of the wound, an analysis of variance of a factor of repeated measurements (ANOVA) was performed; values of $P < 0.05$ were considered statistically significant. In addition, Tukey's and Mann-Whitney of 95% confidence was applied. A statistical analysis was performed on the collected data with PAST3 software.

3. Results

3.1. Anatomical study of V. crocata

The anatomical study of the leaves and stems of *V. crocata* are presented in Table 1 and Fig. 1.

3.1.1. Leaf (Fig. 1B-M)

The anatomical description of the leaves of *V. crocata* is as follows:

Leaf blade: Uniseriate trichomes with 2–5 cells, usually conical in shape; frequently with 1 basal cell (barely up to 3) globose or short cylindrical in shape, further trichomes have the apical cell with different variants; in some cases, this apical cell is evidently narrower than the other ones (acicular). Also, of wide or narrow triangular shape, erect or bent (Fig. 1B–E and G). In superficial view, cells of the adaxial and abaxial epidermis with sinuous walls, those that surround the trichomes have elongated polygonal shapes with thick and straight walls and are formed in a circle up to three rows in a rosette manner (Fig. 1D). Amphistomatic leaves with anomocytic stomata (Fig. 1H) were more abundant on the abaxial surface. In cross section, thin cuticle, smooth on both surfaces; simple epidermis, elliptical to rounded cells, with the external tangential wall more convex than internal tangential. Those that surround the trichomes can be larger and protrude from the rest of the epidermal cells. Small stomata at the same level as the epidermis on both surfaces. Bifacial mesophyll, the palisade parenchyma formed by a single layer of erect and narrow cells, with thin walls, straight to slightly sinuous. The spongy parenchyma with 4 layers; 3 with procumbent cells, tangentially elongated, those of the fourth layer (of the lower surface) erect irregularly, shorter and wider than those of the palisade of the adaxial surface. Collateral vascular bundles are surrounded by parenchymal large cells forming a sheath. Oil-secretory cavities and ducts (Fig. 1F and J). The mesophyll with numerous oil droplets that stain red with Sudan IV. Middle vein (Fig. 1L): With a prominent ridge towards both surfaces (biconvex), a more evident and wide curvature towards the abaxial side; of rounded outline; smooth cuticle on both surfaces; trichomes similar to those described for the lamina, but more abundant and some longer with up to 8 cells and the apical like a whip. In cross-section, both simple epidermis and angular collenchyma below them, more developed towards the adaxial crest (up to 5 layers). The vascular tissue formed by numerous vascular bundles ovate to circular, 3 well developed and up to 7 smaller; all are surrounded by collenchyma that can form a more or less continuous sheath or appear in patches. Two small secretory ducts surrounded by epithelial cells near the central vascular bundle. Petiole (Fig. 1M): In cross-section, it has a half circle outline (flat-convex) with lateral wings. Simple epidermis on both surfaces. Underneath 4–5 layers of angular collenchyma; inward the parenchyma tissue with secretory ducts and cells with sandstone crystals associated with the vascular tissue. With numerous vascular bundles, 3 more developed and several small of different sizes, many of them frequently associate on the side of the xylem of the larger vascular bundles; others are at the base of each wing (one on each base).

3.1.2. Stem (Fig. 1N and O)

The anatomical description of the stems of *V. crocata* is as follows:

In cross section, circular in shape; thin and smooth cuticle. Trichomes like those described for the leaf. Simple epidermis, elliptical shaped cells. In the cortex, there are 4–5 layers of angular collenchyma. Below the second collenchyma layer, a continuous band of peridermis is formed by 3–4 strata, from which 1–2 are phellem with rectangular erect hyaline cells, and the other two layers correspond to phellogen and phelloderm (Fig. 1O). Next, in the innermost collenchyma layers, there are 4–5 strata of parenchyma cells and few ducts surrounded by epithelial cells; inwards an uniestrata sheath (endoderm). In the vascular cylinder, the primary phloem and xylem are still distinguishable, with incipient development of secondary growth of vascular tissues. The secondary phloem surrounded by a continuous band of sclerenchyma that, like the phloem, is better developed in the areas that correspond to the vascular bundles. The secondary xylem continues with projections to the medulla, which correspond to the primary xylem; solitary vessels and grouped in radial chains (Fig. 1N). Wide parenchymatous medulla with circular shape and starry edges.

3.2. Chemical composition

3.2.1. Phytochemical screening

The yield of VcME was 73.7 g (17.3% w/w) and that of VcH was 20.5 g (4.8% w/w). In VcME, terpenes/steroids, alkaloids, phenols

Table 1
Anatomical comparison of *Verbesina* spp. leaf. **1**. *V. crocata*: in this study **2**. *V. encelioides* (Freire et al., 2005). **3**. *V. sordescens* (Castro et al., 1997). **4**. *V. glabrata* (Smiljanic, 2005). **5**. *V. macrophylla* (Bezerra et al., 2018).

Anatomical feature	Species				
	V. crocata (This study)	*V. encelioides* (Freire et al., 2005)	*V. sordescens* (Castro et al., 1997)	*V. glabrata* (Smiljanic, 2005)	*V. macrophylla* (Bezerra et al., 2018)
Anomocytic stomata	++	++	––	++	++
Leaf	A	––	––	H	H
Trichomes	S	S	G	++	S
Secretory cavities	++	––	––	––	++
Number of vascular bundles in the middle vein: principal/smaller	3/up to 7	1–2/–	––	––	5/–
Secretory ducts	3*	–––	1*,2*	2*	3*
Secretory idioblasts	Absent	––	––	––	Absent
Bundle sheath	++	––	––	––	++
Strata number of parenchyma (palisade/spongy)	1/4	––	––	2/2–3	1/3–5
Crystalliferous idioblasts	Sa (In petiole)	––	Absent	P	Absent

A. amphistomatic; H. hypostomatic; S. Simple (uniseriate, uni-multicellular); G. Glandular; 1*. Exclusively associated with the xylem; 2*. Associates with the xylem and phloem; 3*. Exclusively associated with the phloem; P. Prismatic and/or acicular; Sa. Sandstone. ++ Present; –– No information

and glycosides were detected, but not sesquiterpene-lactones. VcH was positive mainly for terpenes/steroids.

3.2.2. HPLC-DAD-ESI/MS of VcH and VcME

3.2.2.1. HPLC-DAD-ESI/MS of VcH. HPLC-ESI/MS analysis identified acetyl-sitosterol (**1**) and its glycoside form (**2**) in the VcH (Fig. 2A). Thus, the sitosterol derivatives presented poor absorbance to UV light, and mass analysis by the total ion current (TIC) is necessary. The molecular ions were detected in the acetylated 457.20 [M + H] and glycosylated forms 577.43 [M+H]. The aglycone part presented one retro-Diels Alder rearrangement (rDA), inducing the ion fragment 279 [M+H]. Other rDA reactions, such as α-cleavage, were observed as double, with the loss of ethylene (28 u) (Fig. 3). The acetylated form showed the loss of acetate (43 u) (data not shown) (SDBS No. 10923, https://sdbs.db.aist.go.jp/sdbs/cgi-bin/direct_frame_top.cgi).

The glycoside showed poor intensity in the spectra. Thus, the ion fragment 415 [M+H] showed breakdown with the aglycone. In addition, four water molecules (72 u) and one oxymethylene were lost. This spectrum was compared to β-sitosterol in the database SDBS (SDBS No. 23321, https://sdbs.db.aist.go.jp/sdbs/cgi-bin/direct_frame_top.cgi) and the NIST (https://webbook.nist.gov/cgi/cbook.cgi?ID=C83465&Units=SI&Mask=200#Mass-Spec). Thus, we can recognize similar ion fragments in both mass spectra at 387, 315, 279, 213, 151, 133, 105, and 80 (*m/z*). *V. crocata* contains acetyl-sitosterol and the glycosylated form.

3.2.2.2. Mass analysis of VcME. In the HPLC-ESI/MS analysis, at least four compounds were identified in VcME: **3**) 2-(3,4-dihydroxyphenyl)-5,7-dihydroxychroman-3-yl-4-(3-amino-4-hydroxyphenyl)-3-hydroxybutanoate; **4**) phylloflavan; **5**) and **6**) two isomers of catechin-3-glycoside (Fig. 2B). This is the first report on catechin

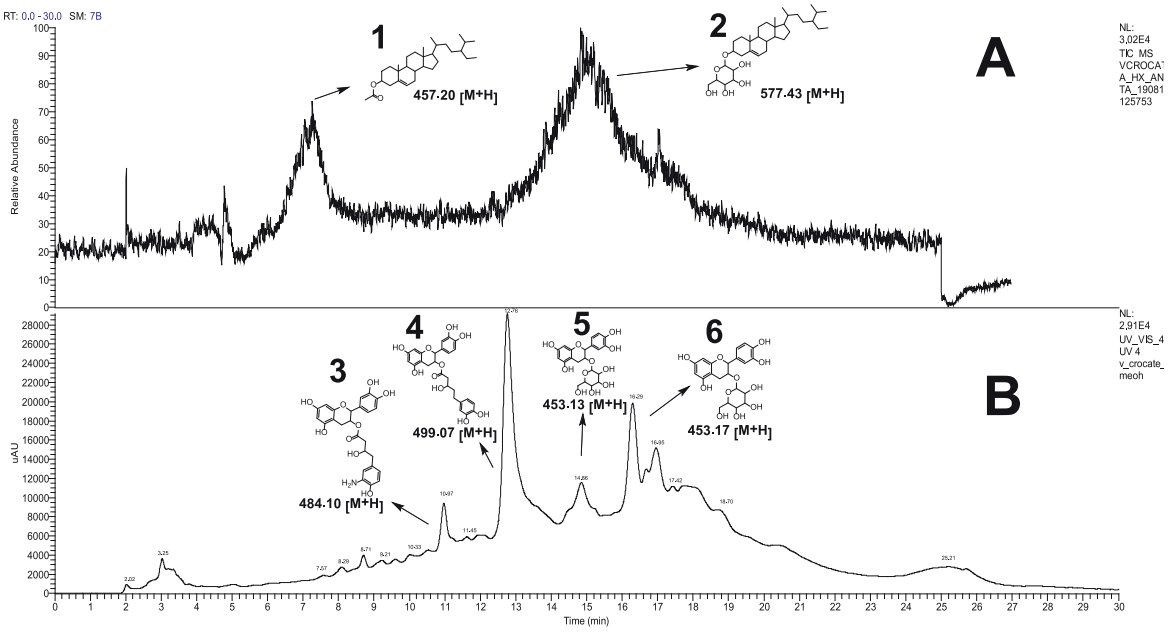

Fig. 2. Chromatogram of the hexanic partition (VcH) and methanolic extract of *V. crocata* (VcME). A) Total ion current (TIC) of VcH. **1**. Acetyl-sitosterol. **2**. Sitosterol glycoside. B) Chromatogram of VcME. **3**. 2-(3,4-dihydroxyphenyl)-5,7-dihydroxychroman-3-yl-4-(3-amino-4-hydroxyphenyl)-3-hydroxybutanoate. **4**. Phylloflavan. **5**. and **6**. Catechin-3-glucoside or glycoside (isomer). UV λ = 254 nm.

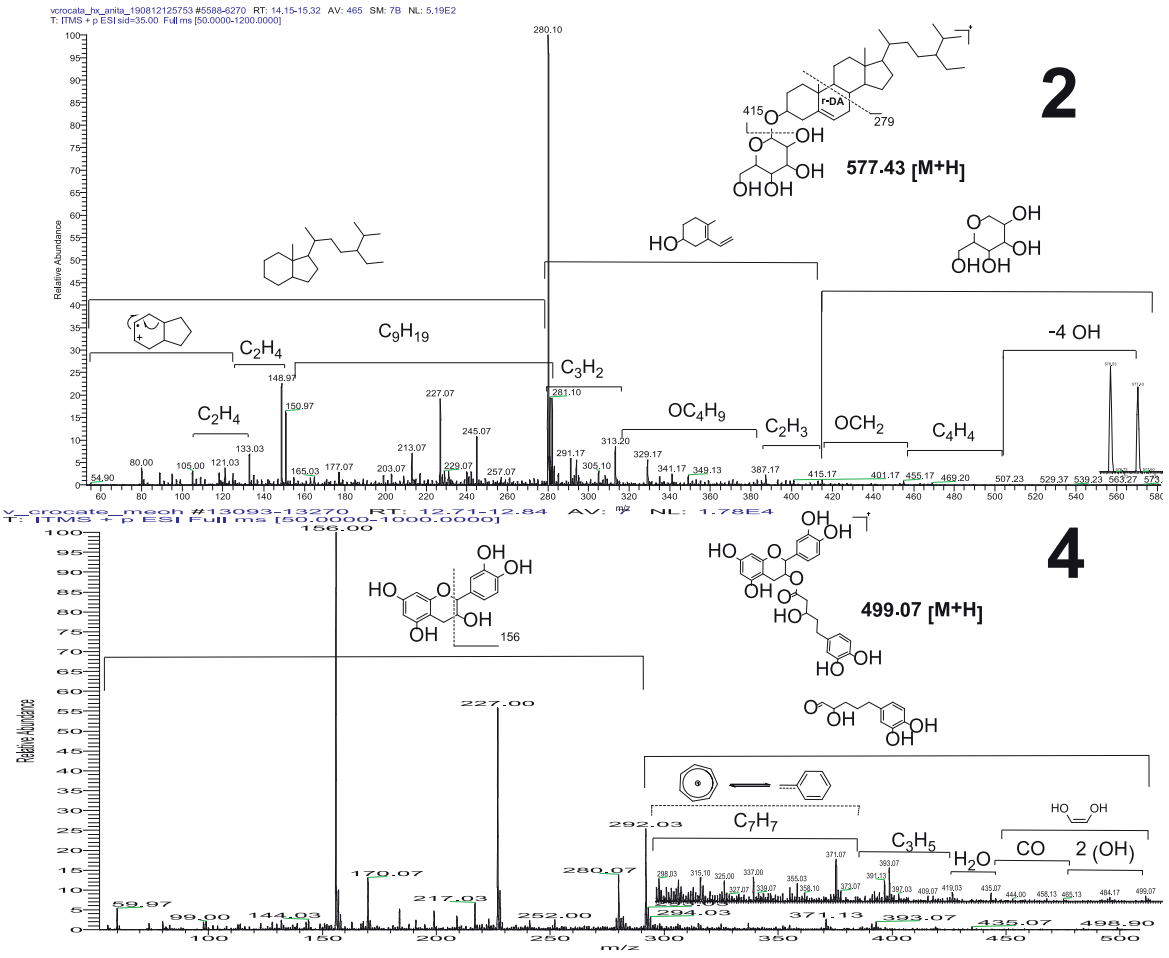

Fig. 3. Full mass spectra of the major compounds detected in *V. crocata*. **2.** Sitosterol glycoside. **4**. Phylloflavan. The mass analyser used was an ion trap with quadrupole isolated, positive mode [M+H]. rDA: *retro*-Diels Alder rearrangement.

derivatives (**3**–**6**) in *V. crocata* and the species of the genus *Verbesina.* Therefore, these derivatives could be considered markers to recognize the plant.

3.2.2.2.1. Analysis of the aglycone catechin by MS. All compounds detected in the VcME have catechin molecules covalently linked to an acid or a monosaccharide. Thus, we analysed the catechin standard by HPLC-ESI/MS to compare the UV absorption spectrum and the fragmentation pattern with that of the VcME analytes. In all cases, the compounds detected in the VcME have the same ion fragments as the catechin standard. Therefore, in both experiments, the ions 56, 60, 73, 80, 89, 97, 102, 114, 123, 128, 139, 149, 156 (base peak BP), 157, 158, 170, 183, 188, 195, 199, 217, 223, 229, 235, 252, 261, 280, 282, 291, and 292 [M+H] are present (data not shown). The ion fragment 156 *m*/*z* is abundant in the catechin standard as well as compounds derived from the catechin. In all molecules, the ion fragment 156 [M+H] was the most intense ion (BP) due to the opening of the C ring, which was induced by the rDA. Therefore, the aglycone part of the molecules is catechin.

3.2.2.2.2. Analysis of the catechin derivatives. Compounds **3** and **4** have an ester linkage at carbon 3 of the catechin molecule. Thus, in **3**, the amine and the hydroxyl of the aromatic ring generated immonium and oxonium ions, which induced the ion fragment 425 [M+H]. Phylloflavan (**4**) generated only oxonium ions, which induced ion fragment 439 [M+H]. In addition, both molecules presented one decarboxylation, the loss of one molecule of water and generated a tropylium ion (91 u) as a β-rupture to the alkyl ligature that induced a McLafferty rearrangement. The fragmentation pattern of compound **4** is presented in Fig. 3, with the ion fragment 227 *m*/*z* [M+H] (60% of abundance). This is fully consistent with the structure of the hydroxypentanoic acid reported by Foo et al. (1985). They isolated the phylloflavan from *Phyllocladus alpinus* (a synonym of *P. trichomanoides* var. *alpinus* (Hook.f.) Parl.) and report the ion fragment 226 *m*/*z*.

Metabolites **5** and **6** are the catechin-3-glycoside isomers (RT 14.86 and 16.29 min, respectively) whit an ether linkage between the monosaccharide and the aglycone. They have similar fragment pathways from ions at 316, 312, 355, 391, 419 and 453 [M+H]. The loss of hydroxyl groups generated oxonium ions as well as the loss of two water molecules (36 u).

Therefore, it is concluded that VcME contains 2-(3,4-dihydroxy phenyl)-5,7-dihydroxychroman-3-yl-4-(3-amino-4-hydroxyphe nyl)-3-hydroxybutanoate (**3**), phylloflavan (**4**) and two catechin-3-glycosides (**5** and **6** isomers).

3.3. DPPH and ABTS radicals-scavenging capacity and total phenol content of VcME

The antioxidant properties and the content of total phenols of the VcME are shown in Table 2. For *V. crocata,* the analysis of its ability to reduce the DPPH radical showed that the VcME had an IC_{50} of 432.56 ± 15.72 μg/mL, while quercetin and catechin had IC_{50} values (5.01 ± 0.01 μg/mL and 6.6 ± 0.25 μg/mL, respectively). A similar effect was observed in the reduction of the ABTS radical. Catechin and quercetin (IC_{50} 6.91 ± 0.03 and 9.16 ± 0.01 μg/mL,

Table 2
Radical scavenging capacity and phenolic content of *V. crocata*.

Test	VcME	Quercetin	Catechin
IC_{50} DPPH (μg/mL)	432.56 ± 15.72*	5.01 ± 0.01	6.6 ± 0.25
IC_{50} ABTS (μg/mL)	1554.57 ± 12.50**	9.16 ± 0.009	6.91 ± 0.03
Phenolic content (mg GAE/ g extract)	19.82 ± 0.77	–	–

Each value corresponds to the average of three different experiments ± SD values; IC_{50} = 50% inhibitory concentration; GAE capacity = gallic acid equivalents; – not determined; *Significant difference with respect to catechin and quercetin ($p = 0.0002$); **Significant difference with respect to catechin and quercetin ($p = 9.34 \times 10^{-14}$).

respectively) have a strong antioxidant potential, while VcME shows lower activity (IC_{50} 1554.57 ± 12.50 μg/mL). The total phenolics in VcME was 19.82 ± 0.77 mg GAE/g extract. The statistical analysis indicates that are not differences between quercetin and catechin ($p = 0.445$ and 0.958) in the reduction of the DPPH and ABTS but exist significant differences between the VcME ($p = 0.0002$ and 9.34×10^{-14}) whit the controls in both tests. The antioxidant activity of the extract was significantly lower compared to flavonoids. However, it is important to consider that catechin and quercetin are pure compounds.

This is the first report on the antioxidant properties and the content of total phenolics in *V. crocata*.

3.4. Wound healing activity

The fast rate of wound closure indicates a better efficacy of treatment. The progressive reduction in the wound area of different groups of animals over 15 days is shown in Fig. 4. The histological diagnosis of wound healing is shown in Figs. 5 and 6.

The initial size of the incisional wound in the CD-1 mice was 15.83 ± 0.54 mm. The FCT in the mice whose incisional wounds were applied VcME was 12 days, while in the groups C- and C+ wound closure did not occur until day 14 (Fig. 4A and B). The above result agrees with the measurements to determine the rate of healing by the wound closing speed (WCS). The fastest wound healing was observed in animals that received VcME, and they had a higher closing speed (1.26 ± 0.90 mm/day) than the C- and C+ groups (1.15 ± 0.47 and 1.17 ± 0.74 mm/day, respectively) (Fig. 4B). The force required to open the wound (g) in the mice in group C- treated with vehicle/Vaseline® was 526 ± 140.3 g. Moreover, the animals to which the Recoveron® (C+) was applied was 640 ± 259.9 g. Finally, the animals treated with VcME needed 700 ± 148.3 g of force to open the wound. A trend was observed, and the topical application of VcME increased the tension force necessary to open the wound, which is greater than with Recoveron® (Fig. 4C). Thus, VcME applied topically to incisional wounds in CD-1 mice accelerates the healing process.

The histological study allowed us to determine that the mice treated with VcME presented a small SHW (80%) in comparison with the C- vehicle (medium-large 40–40%) and C+ Recoveron® (large 60%) groups (Fig. 5).

The histological analysis of the skin sections stained with H&E and MT showed normal epithelialization in the VcME (Fig. 6A) and the C+ Recoveron (Fig. 6B), groups whereas in the C- group hyperplasia was present (80%) (Fig. 6C). In the dermis, little or no granulation of tissue was observed in the VcME and C+ groups, with mature collagen predominating; this was unlike the C- group where there was still granulation tissue, vessel congestion whit immature collagen in the middle area of the wound. In VcME and in C+ regeneration was diagnosed (20%) (Fig. 6B and C, respectively). However, in the case of VcME, the level of organization of the skin was greater, with the presence of glands, hair follicles and mature collagen. Finally, animals treated with VcME have significantly less fibroblasts by mouse in the area of the unhealed wound (189 ± 22.03; $p = 0.0367$) than those treated with Vaseline® (327.6 ± 39.37). Recoveron® group had 257.8 ± 38.24 fibroblasts/mouse (Fig. 6D).

In the case of animals treated with Vaseline®, they were between the stages of inflammation and proliferation according to the histological diagnosis. Those treated topically with Recoveron® were in the final proliferative stage and beginning the remodelling phase. In the case of treatment with VcME, it was determined that there were also indications of the proliferation phase. However, the phase of remodelling is more advanced in terms of the synthesis of mature collagen and the number of fibroblasts. These results indicate that the topical application of

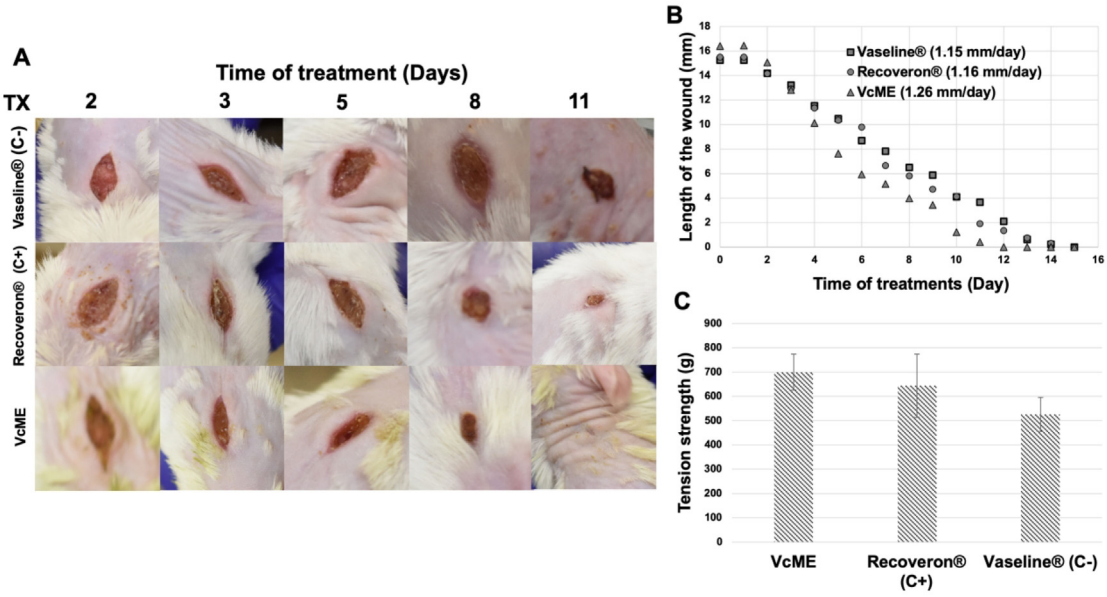

Fig. 4. Wound healing activity of *V. crocata* methanolic extract (VcME). (A) Photographic selection of wound closure on different post-excision days; (B) Wound closure speed (WCS mm/day); and (C) Tension strength (g). These data were obtained at the end of the treatment application time (14 days after incision). The data are represented as the means ± S.E. (n = 5).

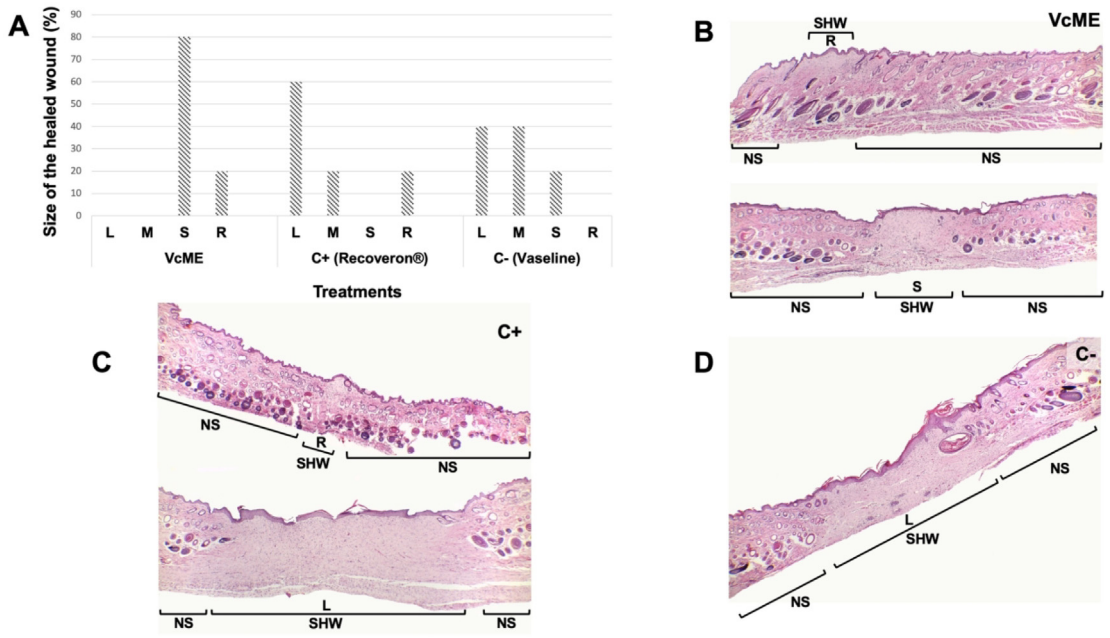

Fig. 5. (A) Size of the healed wound of mice treated with *V. crocata* (VcME), C+ (Recoveron®) and C- (Vaseline®). (B–D) Representative images of H&E staining sections of the wounds of each treatment. NS. normal skin; L. large; R. regeneration; S. small; SHW. size of the healed wound.

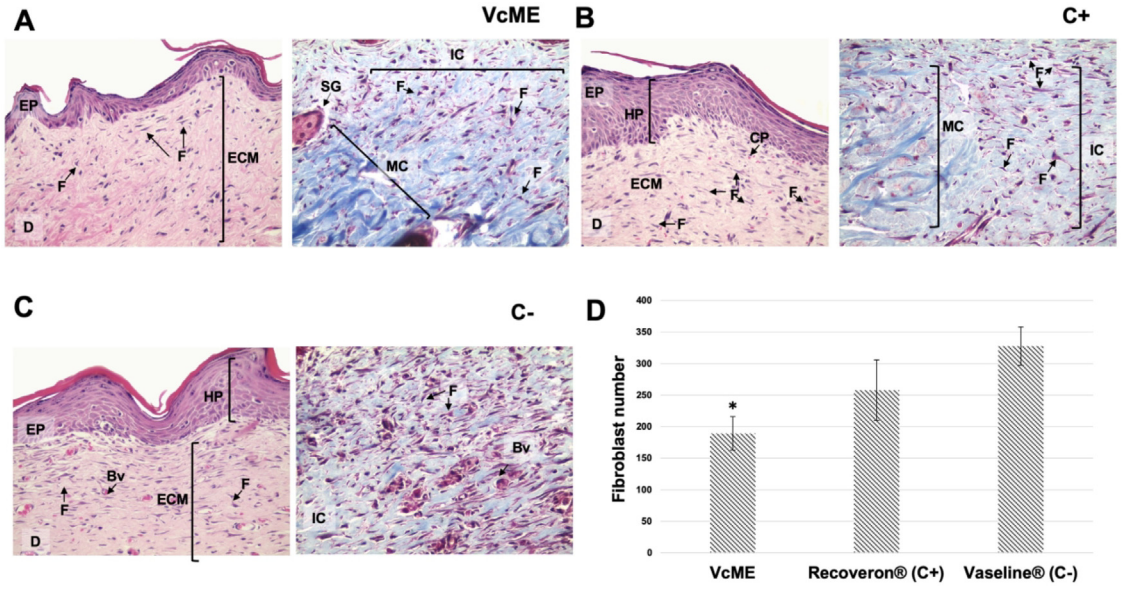

Fig. 6. Representative images of the histological analysis of H&E and MT staining sections of the wounds of each treatment. (A) treatment with *V. crocata* (VcME); (B) Positive control: Recoveron® (C+); (C) Negative control: Vaseline® (C-); (D) Fibroblast number/mouse in each group. *Significant difference with respect to Vaseline® treatment ($p = 0.0367$). Bv. blood vessel; Cp. capillary; D. dermis; ECM. extracellular matrix; EP. epidermis; F. fibroblast, HP. hyperplasia; IC. immature collagen; MC. mature collagen; SG. sebaceous gland.

V. crocata accelerates the healing process by reducing the time of wound closure and promotion of cutaneous reorganization.

4. Discussion

4.1. Anatomical study

Plant anatomy, as an integral part of pharmacognosy studies, has the purpose of providing data to allow the recognition of a species with medicinal importance because the plant tissues contain the active ingredients that provide the plant's pharmacological effect (Dickison, 2000; Chanda, 2014).

Of the genus *Verbesina*, 119–180 species have been registered in Mexico (Harker and Jiménez-Reyes, 2002; Villaseñor, 2004, 2018), of which there are no anatomical studies focused on the attribute of the plant or as part of the pharmacognosis. Studies conducted on *V. macrophylla* (Cass.) S.F.Blake, native of Brazil (Bezerra et al., 2018), and *V. encelioides* (Cav.) Benth. & Hook.f. ex A.Gray from Argentina (Freire et al., 2005), show differences in some characters of the leaves with respect to *V. crocata* (Table 1).

For the stems, there is no comparison with other *Verbesina* species. The main differences and those which can potentially have taxonomic significance in the species separation reside in the characteristics of leaves, some of these are: the anticlinal walls of the adaxial epidermal cells, the presence of stomata on one or both surfaces, the types and abundance of trichomes in some of the leaf surfaces and the number of vascular bundles of the middle vein, which appear to be more numerous in *V. crocata* (taking into account the totality of vascular bundles) than in *V. macrophylla* and in *V. encelioides* (Table 1), which are recorded with 5 and 1–2, respectively.

Although ducts and secretory cavities are recorded in numerous species of Asteraceae (Castro et al., 1997; Bezerra et al., 2018; Smiljanic, 2005), it seems that their position, characteristics and/or sizes differ among them. For the case of *V. crocata*, the ducts are small and associated with vascular bundles in the middle vein and petiole; they are scarcely distinguishable and extremely scarce in the leaf blade compared with *V. macrophylla*, as well as with species of other genera (Milan et al., 2006). The presence and absence of the various types of secretory structures and their position on the leaves are used for diagnostic value (Castro et al., 1997). Finally, the characters of the middle vein and trichomes are potentially useful for the recognition of *V. crocata*.

4.2. Chemical composition of V. crocata

The phytochemical screening of *V. crocata* indicates that it contains terpenes/steroids, alkaloids, phenols and glycosides. The presence of terpenes and steroids in *V. crocata* is consistent with the results reported in the review by Mora et al. (2013). They mentioned that a group of secondary metabolites characteristic of the genus *Verbesina* are terpenoids. In VcH, sitosterol derivatives were detected by HPLC-ESI/MS. Regarding alkaloids, different types have been reported in some species of the genus, such as galegine in *V. encelioides* and caracasanamide in *V. caracasan*a B.L.Rob. & Greenm. Also, some phenolic compounds have been described in the genus, such as syringic acid in *V. sublobata* Benth. and *V. myriocephala* Sch. Bip. ex Klatt, ferulic acid in *V. gigantea* Jacq., p-coumaric acid in *V. myriocephala* and *V. virginica* L. (Herz and Kumar, 1981), rhamnocitrin-3-glucuronide in *V. myriocephala* (Wagner et al., 1974) and glycosides of quercetin in *V. encelioides* (Glennie and Jain, 1980). Also, in this work the presence of glycosylated derivatives of the catechin was determined (**3**–**6**).

Sitosterol glycoside (**2**) is the main component of VcH. β-Sitosterol glucoside and β-sitosterol galactoside were isolated from the petroleum ether fraction of *V. encelioides* (Tiwari et al., 1978; Jain et al., 2008a; Abbas et al., 2016; Ezzat et al., 2017). It has been reported that sitosterol and sitosterol glycoside presented anti-inflammatory, anti-neoplastic, anti-pyretic, and immune-modulatory activity. Their mixture seems to target specific T-helper lymphocytes, TH1 and TH2 cells, helping to normalize their function and resulting in improved T-lymphocyte and natural killer cell activity (Bouic and Lamprecht, 1999). β-Sitosterol-β-D-gluco side isolated from *Trachelospermum jasminoides* (Lindl.) Lem. has an anti-inflammatory effect. This metabolite reduced the NO production (72.8%) and the secretion of pro-inflammatory cytokines such as TNF-α (23.3%), IL-6 (64.1%) and IL-1β (46.7%) in RAW 264.7 cells (Choi et al., 2012). β-Sitosterol glucoside exhibited anti-inflammatory and pain killing action *in vitro* by downregulating cell-signalling pathway mediators such as TNF-α, COX-2, IL-6, MMP-13 and protein denaturation. Also, *in vivo* reduced the acute inflammation induced by carrageenan in the rat paw oedema model (Das et al., 2018).

Phylloflavan is the main component of VcME (**4**), an acetylated flavan-3-ol, has been reported in *P. alpinus* (Foo et al., 1985) and in *P. trichomanoides* (Foo, 1987). This compound has antileishmanial activity *in vitro* in intracellular amastigotes of *Leishmania donovani* (EC_{50} 3.2 nM); but is inactive in extracellular promastigotes (EC_{50} 50.2 nM); and activated the RAW 264.7 macrophage cell line and cause the moderate release of NO (8 mM) by the stimulation of IFN-γ/LPS (119 mM). Thus, phylloflavan might be considered a beneficial immunological response modifier (Kolodziej et al., 2001).

Compounds **5** and **6** are catechin glycosides. However, to establish the type of sugar attached to the skeleton of the aglycone, it is necessary to isolate these isomers and elucidate their structure by other methods. Although flavonoid glycosides have been previously reported in some species. Several quercetin glycosides in *V. encelioides* have been identified (Glennie and Jain, 1980). *V. myriocephala* contains the flavonol rhamnocitrin-3-glucuronide (Wagner et al., 1974).

4.3. Antioxidant activity

V. crocata has low antioxidant activity against DPPH and ABTS radicals and total phenolics. This coincides with other species of the genus, such as *V. encelioides*, it was determined that at 80 μg/mL, a DPPH reduction of 20% was obtained, but these authors did not evaluate the IC_{50} (Jain et al., 2008b). The above result correlates with the content of total phenolics. The total phenolics for VcME is within the range reported for extract *V. encelioides* in leaves (22.5 mg GAE/g) and in stems (18.31 mg GAE/g) (Jain et al., 2008b). In general, the antioxidant activity of the species of the genus *Verbesina* is low. There are no reports on antioxidant activity against the radical ABTS of some *Verbesina* species.

4.4. Wound healing activity

According to our results, *V. crocata* favours the wound healing process. This supports the traditional use of this species in San Rafael Coxcatlán, Puebla, Mexico (Canales et al., 2005) as well as in other parts of the country (Pérez et al., 1984; Alonso-Castro et al., 2011; Vibrans, 2011).

The topical application of VcME showed an improvement in the healing process of incisional wounds in CD-1 mice, increasing the WCS and the tension force required to open the wound (Fig. 4). This is consistent with the histological study, because topical application of VcME promotes the synthesis and organization of collagen, and significantly decreases the number of fibroblasts, to reach the proliferation/remodelling phases after 15 days (Fig. 5). The contraction of the wound indicates a reduction in the unhealed area during the healing process. This involves the gradual degradation of the immature collagen until the maturation of the collagen fibres, the establishment of the newly formed epithelium and the possible regeneration of cutaneous components for the recovery of function (Reinke and Sorg, 2012). In this process the fibroblasts participate in breaking down the fibrin clot, synthesis of ECM and collagen structures to support the other cells associated with effective wound healing (Bainbridge, 2013). Subsequently, the synthesis of collagen increases throughout the wound, while the proliferation of fibroblasts declines as the process progresses to the remodelling phase (Reinke and Sorg, 2012).

The beneficial effect of *V. crocata* could be attributed to its chemical composition; several of its components are anti-inflammatory. This property can favour the wound healing process. The aqueous extract of *V. crocata* has anti-inflammatory activity with the model of induction of plantar oedema by carrageenan in CD-1 mice (Rodríguez, 2014). In this study, the phytochemical screening of VcME and VcH was positive for terpenes. Dalla Via et al. (2015) showed that two eudesmane-type sesquiterpenes from the hexanic extract of *V. persicifolia* DC. have anti-inflammatory properties in a murine model of atrial oedema

induced by TPA. Additionally, we found that the main constituent of VcH was sitosterol glycoside. This compound has anti-inflammatory activity in both *in vitro* and *in vivo* tests (Choi et al., 2012; Das et al., 2018). In addition, we determined that VcME contains phylloflavan. This compound activates macrophages and could participate in the modulation of the immune response (Kolodziej et al., 2001). VcME has low antioxidant activity, so it might decrease the formation of ROS in the wound area, avoiding complications from oxidative stress.

Thus, the topical application of *V. crocata* could decrease inflammation, modulate the immune response and therefore improve the wound healing process. This is consistent with the traditional use of the plant in Mexico. However, it is still necessary to isolate the active principles of the plant and study its mechanisms of action.

5. Conclusions

The pharmacognostic study of *V. crocata* allowed us to determine that the catechin derivatives, the characteristics of the middle vein and trichomes, are potentially useful for the recognition of the plant. Additionally, the topical application of *V. crocata* accelerates the wound healing process by reducing the time to close the wound, increasing the wound closing speed and tension force, as well as presenting a small size of the healed wound with normal epithelization in the dermis without evidence of inflammatory processes, reorganization of mature collagen and decrease in the number of fibroblasts reaching the remodelling phase.

Author contributions

GBAM and ASN conceived, designed and performed the experiments. LVME, JRMP, ARS, and GVD performed the analysis of plant anatomy. HDCT, EPA and EGAM performed the chemical study. SPR and ASN carried out the studies of the antioxidant and wound healing activities. GVMR, BFJC and ASN performed the histological analysis. GBAM and ASN wrote the manuscript and analysed the statistical data. All authors read and approved the final manuscript.

Declaration of Competing Interest

The authors declare that they have no known competing financial interests or personal relationships that could have appeared to influence the work reported in this paper.

Acknowledgements

We express our gratitude to Lt. Col. José Cruz Rivera Cabrera, Chief Department of Pharmacology, Unit of LC-MS, Escuela Médico Militar, México; and Leticia Flores Sánchez and Tomás E. Villamar Duque from the FES-Iztacala, UNAM Bioterium.

Funding

This work was supported by DGAPA, PAPIIT-UNAM (Grant IN-215017) and Programa de Becas Postdoctorales-UNAM (041/2017 UNAM-DGAPA); Posgrado en Ciencias Biológicas-UNAM and Beca de Maestría-CONACYT (CVU 775307).

References

Abbas, F.A., El Sayed, Z.I., Dora, G.A., Ateya, A.M., Samy, S., 2016. Phytochemical and biological studies of *Verbesina encelioides* (Cav.) Benth. and Hook. AJPCR 4, 108–120.

Aguilar-Rodríguez, S., 1998. Apéndice I. Técnicas de laboratorio para el estudio de las embriofitas. En: Tejero-Díez, J.D., Granillo, V.M.P. (Eds.) Plantae. Introducción al Estudio de las Plantas con Embrión. Universidad Nacional Autónoma de México, Facultad de Estudios Superiores Iztacala, pp. 247-272.

Ali, S., Khan, M.R., Batool, R., Maryam, S., Majid, M., 2019. Wound healing potential of oil extracted from *Parrotiopsis jacquemontiana* (Decne) Rehder. J. Ethnopharmacol. 236, 354–365. https://doi.org/10.1016/j.jep.2019.03.018.

Alonso-Castro, A.J., Villarreal, M.L., Salazar-Olivo, L.A., Gomez-Sanchez, M., Dominguez, F., Garcia-Carranca, A., 2011. Mexican medicinal plants used for cancer treatment: pharmacological, phytochemical and ethnobotanical studies. J. Ethnopharmacol. 133, 945–972. https://doi.org/10.1016/j.jep.2010.11.055.

Andrade-Cetto, A., Heinrich, M., 2005. Mexican plants with hypoglycaemic effect used in the treatment of diabetes. J. Ethnopharmacol. 99, 325–348. https://doi.org/10.1016/j.jep.2005.04.019.

Bainbridge, P., 2013. Wound healing and the role of fibroblasts. J. Wound Care 22, 407–412 https://doi.org/10.12968/jowc.2013.22.8.407.

Bezerra, L.D.A., Mangabeira, P.A.O., de Oliveira, R.A., Costa, L.C.D.B., Da Cunha, M., 2018. Leaf blade structure of *Verbesina macrophylla* (Cass.) F. S. Blake (Asteraceae): ontogeny, duct secretion mechanism and essential oil composition. Plant. Biol. (Stuttg) 20, 433–443. https://doi.org/10.1111/plb.12700.

Block, L.H., 2013. Medicated topicals. In: Felton, L. (Ed.), Remington: Essentials of Pharmaceutics. Pharmaceutical Press, London, pp. 571–572.

Biswas, T.K., Pandit, S., Chakrabarti, S., Banerjee, S., Poyra, N., Seal, T., 2017. Evaluation of *Cynodon dactylon* for wound healing activity. J. Ethnopharmacol. 197, 128–137. https://doi.org/10.1016/j.jep.2016.07.065.

Bouic, P.J., Lamprecht, J.H., 1999. Plant sterols and sterolins: a review of their immune-modulating properties. Altern Med Rev. 4, 170–177.

Canales, M., Hernández, T., Caballero, J., Romo de Vivar, A., Avila, G., Duran, A., Lira, R., 2005. Informant consensus factor and antibacterial activity of the medicinal plants used by the people of San Rafael Coxcatlán, Puebla, México. J. Ethnopharmacol. 97, 429–439. https://doi.org/10.1016/j.jep.2004.11.013.

Castro, M.M., Leitão-Filho, H., Monteiro, W., 1997. Utilização de estruturas secretoras na identificação dos gêneros de Asteraceae de uma vegetação de cerrado. Revta. Brasil. Bot. São Paulo 20, 163–174. https://doi.org/10.1590/S0100-84041997000200007.

Chanda, S., 2014. Importance of pharmacognostic study of medicinal plants: an overview. J. Pharmacogn. Phytochem. 2, 69–73.

Chew, A.L., Maibach, H. 2006. 54 In vitro methods to predict skin irritation. In: Chew, A Chew, A.L., Maibach, H. (Eds). Irritant dermatitis. Springer. pp. 501–508.

Chitra, S., Patil, M.B., Ravi, K., 2009. Wound healing activity of *Hyptis suaveolens* (L.) poit (Lamiaceae). Int. J. Pharm. Tech. Res. 1, 737–744.

Choi, J.N., Choi, Y.H., Lee, J.M., Noh, I.C., Park, J.W., Choi, W.S., Choi, J.H., 2012. Anti-inflammatory effects of β-sitosterol-β-D-glucoside from *Trachelospermum jasminoides* (Apocynaceae) in lipopolysaccharide-stimulated RAW 264.7 murine macrophages. Nat. Prod. Res. 26, 2340–2343. https://doi.org/10.1080/14786419.2012.654608.

Dalla Via, L., Mejia, M., García-Argáez, A.N., Braga, A., Toninello, A., Martínez-Vázquez, M., 2015. Anti-inflammatory and antiproliferative evaluation of 4β-cinnamoyloxy,1β,3α-dihydroxyeudesm-7,8-ene from *Verbesina persicifolia* and derivatives. Bioorg. Med. Chem. 23, 5816–5828. https://doi.org/10.1016/j.bmc.2015.07.002.

Das, N., Bhattacharya, A., Kumar, M.S., Debnath, U., Dinda, B., Mandal, S.C., Kumar, S. P., Kumar, A., Dutta, C.M., Maiti, S., Palit, P., 2018. *Ichnocarpus frutescens* (L.) R. Br. root derived phyto-steroids defends inflammation and algesia by pulling down the pro-inflammatory and nociceptive pain mediators: an *in-vitro* and *in-vivo* appraisal. Steroids 139, 18–27. https://doi.org/10.1016/j.steroids.2018.09.005.

Dickison, W.C., 2000. Integrative Plant Anatomy. Academy Press, California.

Dwita, L.P., Hasanah, F., Srirustami, R., Repi, Purnomo, R., Harsodjo, S. 2019. Wound healing properties of Epiphyllum oxypetalum (DC.) Haw. leaf extract in streptozotocin-induced diabetic mice by topical application. Wound Med. 26, 100160. https://doi.org/10.1016/j.wndm.2019.100160.

Ezzat, S.M., Salama, M.M., Mahrous, E.A., Maes, L., Pan, C.H., Abdel-Sattar, E., 2017. Antiprotozoal activity of major constituents from the bioactive fraction of *Verbesina encelioides*. Nat. Prod. Res. 31, 676–680. https://doi.org/10.1080/14786419.2016.1180604.

Fahn, A., 1985. Anatomía Vegetal. Pirámide, Madrid, España.

Foo, L.Y., 1987. Phenylpropanoid derivatives of catechin, epicatechin and phylloflavan from *Phyllocladus trichomanoides*. Phytochemistry 26, 2825–2830. https://doi.org/10.1016/S0031-9422(00)83598-0.

Foo, L.Y., Hrstich, L., Vilain, C., 1985. Phylloflavan, a characteristic constituent of *Phyllocladus* species. Phytochemistry 24, 1495–1498. https://doi.org/10.1016/S0031-9422(00)81052-3.

Freire, E.S., Arambarri, M.A., Bayón, D.N., Sancho, G., Urtubey, E., Monti, C., Novoa, C. M., Colares, N.M., 2005. Epidermal characteristics of toxic plants for cattle from the Salado river basin (Buenos Aires, Argentina). Bol. Soc. Argent. Bot. 40, 241–281.

Gantwerker, E.A., Hom, D.B., 2012. Skin: Histology and physiology of wound healing. Clin. Plast. Surg. 39, 85–97. https://doi.org/10.1016/j.cps.2011.09.005.

Gautam, A., Jhade, D., Ahirwar, D., Sujane, M., Sharma, G.N., 2010. Pharmacognostic evaluation of *Toona ciliata* bark. J. Adv. Pharm. Technol. Res. 1, 216–220.

Glennie, C.W., Jain, S.C., 1980. Flavonol 3,7-diglycosides of *Verbesina encelioides*. Phytochemistry 19, 157–158. https://doi.org/10.1016/0031-9422(80)85040-0.

Gupta, N., Jain, U.K., 2011. Investigation of wound healing activity of methanolic extract of stem bark of *Mimusops elengi* Linn. Afr. J. Tradit. Complement. Altern. Med. 8, 98–103. https://doi.org/10.4314/ajtcam.v8i2.63197.

Harker, M., Jiménez-Reyes, N., 2002. *Verbesina barrancae* (Compositae, Heliantheae), a new species from Jalisco, Mexico. Brittonia 54, 181–189. https://doi.org/10.1663/0007-196X(2002)054[0181:VBCHAN]2.0.CO;2.

Herz, W., Kumar, N., 1981. Aromatic and other constituents of four *Verbesina species*: Structure and stereochemistry of verbesindiol. Phytochemistry 20, 247–250. https://doi.org/10.1016/0031-9422(81)85100-X.

Jain, S.C., Jain, R., Singh, R., Menghani, E., 2008a. *Verbesina encelioides*: perspective and potentials of a noxious weed. IJTK 7, 511–513.

Jain, S.C., Singh, R., Jain, R., 2008b. Antimicrobial and antioxidant potentials of *Verbesina encelioides* (Cav.) Benth. and Hook. Fil ex Gray. J. Med. Plant. 2, 61–65. https://doi.org/10.3923/rjmp.2008.61.65.

Johansen, D.A., 1940. Plant Microtechnique. Mc.Graw-Hill, Nueva York.

Kolodziej, H., Kayser, O., Kiderlen, A.F., Ito, H., Hatano, T., Yoshida, T., Foo, L.Y., 2001. Proanthocyanidins and related compounds: antileishmanial activity and modulatory effects on nitric oxide and tumor necrosis factor-alpha-release in the murine macrophage-like cell line RAW 264.7. Biol. Pharm. Bull. 24, 1016–1021. https://doi.org/10.1248/bpb.24.1016.

Kumar, B., Vijayakumar, M., Govindarajn, R., Pushpangadan, P., 2007. Ethno-pharmacological approaches to wound healing-exploring medicinal plants of India. J. Ethnopharmacol. 114, 103–113. https://doi.org/10.1016/j.jep.2007.08.010.

Landén, N.X., Li, D., Ståhle, M., 2016. Transition from inflammation to proliferation: a critical step during wound healing. Cell. Mol. Life Sci. 73, 3861–3885. https://doi.org/10.1007/s00018-016-2268-0.

López-Alarcón, C., Denicola, A., 2013. Evaluating the antioxidant capacity of natural products: a review on chemical and cellular-based assays. Anal. Chim. Acta 763, 1–10. https://doi.org/10.1016/j.aca.2012.11.051.

Mandalari, G., Tomaino, A., Arcoraci, T., Martorana, M., Lo Turco, V., Cacciola, F., Rich, G.T., Bisignano, C., Saija, A., Dugo, P., Cross, K.L., Parker, M.L., Waldron, K.W., Wickham, M.S.J., 2010. Characterization of polyphenols, lipids and dietary fibre from almond skins (*Amygdalus communis* L.). J. Food Compos. Anal. 23, 166–174. https://doi.org/10.1016/j.jfca.2009.08.015.

Marles, R.J., Farnsworth, N.R., 1995. Antidiabetic plants and their active constituents. Phytomedicine 2, 137–189. https://doi.org/10.1016/S0944-7113(11)80059-0.

Metcalfe, C.R.C., Chalk, L., 1950. Anatomy of the dicotyledons: Leaves, stem, and wood in relation to taxonomy, with notes on economic uses. vol. 2. Clarendon Press, Oxford.

Metcalfe, C.R.C., Chalk L., 1979. Anatomy of the dicotyledons. Vol. 1. second ed. Clarendon Press, Oxford.

Milan, P., Hayashi, A.H., Appezzato-da-Glória, B., 2006. Comparative leaf morphology and anatomy of three Asteraceae Species. Braz. Arch. Biol. Technol. 49, 135–144. https://doi.org/10.1590/S1516-89132006000100016.

Mora, F.D., Alpan, L., McCracken, V.J., Nieto, M., 2013. Chemical and biological aspects of the genus *Verbesina*. Nat. Prod. J. 3, 140–150. https://doi.org/10.2174/2210315511303020009.

NIST, 2017. National Institute of standards and technology. https://webbook.nist.gov/cgi/cbook.cgi?ID=C83465&Units=SI&Mask=200#Mass-Spec. (accessed 20 June 2019).

Olsen, 1988. A revision of Verbesina section Platypteris (Asteraceae: Heliantheae). SIDA. 13, 45–56.

Pérez, R.M., Ocegueda, A., Muñoz, J.L., Avila, J.G., Morrow, W.W., 1984. A study of the hypoglycemic effect of some Mexican plants. J. Ethnopharmacol. 12, 253–262. https://doi.org/10.1016/0378-8741(84)90054-0.

Re, R., Pellegrini, N., Proteggente, A., Pannala, A., Yang, M., Rice-Evans, C.A., 1999. Antioxidant activity applying an improved ABTS radical cation decolorization assay. Free Radic. Biol. Med. 26, 1231–1237. https://doi.org/10.1016/S0891-5849(98)00315-3.

Reinke, J.M., Sorg, H., 2012. Wound repair and regeneration. Eur. Surg. Res. 49, 35–43. https://doi.org/10.1159/000339613.

Rodríguez, A.L.H., 2014. Evaluación de la actividad antiinflamatoria del extracto acuoso de Verbesina crocata (Cav.) Less. (Capitaneja). FES-Zaragoza. UNAM Master's Thesis of Science. México.

Rozaini, M.Z., Zuki, A.B.Z., Noordin, M., Norimah, Y., Hakim, A.N., 2004. The effects of different types of honey on tensile strength evaluation of burn wound tissue healing. Int. J. Appl. Res. Vet. Med. 2, 290–296.

Ruzin, S.E., 1999. Plant Microtechnique and Microscopy. Oxford University Press, New York, USA.

Salazar-Gómez, A., Pablo-Pérez, S.S., Estévez-Carmona, M.M., Meléndez-Camargo, M.E., 2018. Diuretic activity of aqueous extract and smoothie preparation of *Verbesina crocata* in rat. Bangladesh. J. Pharmacol. 13, 236–240. https://doi.org/10.3329/bjp.v13i3.27584.

Sathyanarayanan, S., Muniyandi, K., George, E., Sivaraj, D., Sasidharan, S.P., Thangaraj, P., 2017. Chemical profiling of *Pterolobium hexapetalum* leaves by HPLC analysis and its productive wound healing activities in rats. Biomed. Pharmacother. 95, 287–297. https://doi.org/10.1016/j.biopha.2017.08.062.

SDBS (SDBS No. 10923) https://sdbs.db.aist.go.jp/sdbs/cgi-bin/direct_frame_top.cgi (accessed 20 June 2019).

SDBS (SDBS No. 23321) https://sdbs.db.aist.go.jp/sdbs/cgi-bin/direct_frame_top.cgi (accessed 20 June 2019).

Smiljanic, K.B.A., 2005. Anatomia foliar das espécies de Asteraceae em um afloramento rochoso no parque estadual da Serra do Brigadeiro (MG). Universidade Federal de Viçosa. Masteŕs Thesis of Science. Minas Gerais, Brasil. 92p http://lattes.cnpq.br/8320644446637344.

Song, Y., Zeng, R., Hu, L., Maffucci, K.G., Ren, X., Qu, Y., 2017. *In vivo* wound healing and *in vitro* antioxidant activities of *Bletilla striata* phenolic extracts. Biomed. Pharmacother. 93, 451–461. https://doi.org/10.1016/j.biopha.2017.06.079.

Tiwari, H., Rao, P., Sambasiva, V., 1978. Constituents of *Verbesina encelioides*: Isolation of triterpenoids from a Verbesina species. Indian J. Chem. 16, 1133.

The Plant List, 2013. http://www.theplantlist.org/tpl1.1/search?q=Verbesina+crocata. (accesed 20 june 2019).

Vibrans, H. 2011. Malezas de México Verbesina crocata (Cav.) Less. Comisión Nacional Para El Conocimiento y Uso De La Biodiversidad, México. http://www.conabio.gob.mx/malezasdemexico/asteraceae/verbesina-crocata/fichas/ficha.htm (accessed 20 June 2019).

Villaseñor, J.L., 2004. Los géneros de plantas vasculares de la flora de México. Bol. Soc. Bot. Méx. 75, 105–135.

Villaseñor, J.L., 2018. Diversidad y distribución de la familia Asteraceae en México. Bot. Sci. 96, 332–358 http://doi.org/10.17129/botsci.1872.

Wagner, H., Iyengar, M.A., Seligmann, O., Herz, W., 1974. Rhamnocitrin-3-glucuronid in *Verbesina myricephala*. Phytochemistry 13, 493–494. https://doi.org/10.1016/S0031-9422(00)91241-X.

Wang, P.H., Huang, B.S., Horng, H.C., Yeh, C.C., Chen, Y.J., 2018. *Wound healing*. J. Chin. Med. Assoc. 81, 94–101. https://doi.org/10.1016/j.jcma.2017.11.002.